SCIENCE CHINA
Chemistry

• ARTICLES •

June 2012 Vol.55 No.6: 1167–1174
doi: 10.1007/s11426-012-4594-x

Preparation and synergetic catalytic effects of amino-functionalized MCM-41 catalysts

LANG WanZhong*, SU Bo, GUO YaJun* & CHU LianFeng

Key Laboratory of Resource Chemistry of Ministry of Education; Shanghai Key Laboratory of Rare Earth Functional Materials; College of Life and Environmental Science, Shanghai Normal University, Shanghai 200234, China

Received April 28, 2011; accepted November 5, 2011; published online May 21, 2012

Four amine functionalized mesoporous catalysts were synthesized by grafting primary, dualistic and two secondary amines onto the channel walls of mesoporous silica, MCM-41. We examined the effects of organoamine loading amount on the acid-base synergism of the catalysts in the self-condensation reaction of *n*-butanal, a Knoevenagel condensation and a Henry reaction. We observed the balance of the amine and residual silanol amounts is crucial to the catalytic performances of the functionalized mesoporous catalysts. An optimum organoamine loading amount exists, which is dependent on the organoamine type. There is little difference in the optimum organoamine loading amount between different reactions. The secondary organoamine functionalized MCM-41 exhibits the best catalytic performance in the experimental range.

MCM-41, acid-base synergism, organoamine, *n*-butanal

1 Introduction

Since the discovery in 1992 [1], mesoporous silica has been widely used as a host for catalytic moieties such as basic [2–4] and acidic [5–7] groups to form active heterogeneous nano catalysts. One important method to prepare mesoporous catalysts is to introduce reactive organic groups into the pores of mesoporous silica [8–13]. Among the mesoporous catalysts, amino-functionalized mesoporous materials used as heterogenous catalysts have attracted more attention. The catalytic performances of the amino-functionalized mesoporous catalysts have been investigated for carbon-carbon coupling reactions [14–27], including knoevenagel condensation reaction and aldol condensation reaction.

In previous reports, the catalytic activity of the amino-functionalized mesoporous catalysts was evaluated either upon equal catalyst mass [24] or upon equal mole amine [28]. However, recent investigations showed that the surface silanols of the mesoporous silica were beneficial to the catalytic performances for the synergetic catalytic effects with the introduced reactive groups like amines [29–34]. Hruby *et al.* [33] claimed that the residual silanols may transfer a proton for its weakly acidic quality. Such synergetic acid-base catalytic mechanism was also proposed for aminopropyl-functionalized silica gel for Henry reaction [29]. Due to the existence of silanol-amine acid-base synergetic effect, the balance between amine and silanol groups in amount needs to be considered when the catalytic activities of the functionalized catalysts were evaluated. Besides the residual silanols, several acidic groups were introduced to substitute silanols and enhance the synergetic catalytic effects of the amino-functionalized mesoporous silica [35–41]. However, in comparison with strong acidic groups, the surface silanol groups with mildly acidic property exhibited better synergetic catalysis performances in aldol reactions [34]. Sharma *et al.* [32] synthesized primary amine functionalized mesoporous silica with different amine densities by grafting aminoorganosilanes. The synergetic catalytic performances of the catalysts were evalu-

*Corresponding author (email: wzlang@shnu.edu.cn; guoyajun2000@yahoo.com,cn)

ated for Henry reaction. They found the catalysts with 0.8–1.5 mmol organoamine/g had the best silanol-amine synergetic catalytic activity, which was dubbed as the critical density of the grafted organic groups. Regretfully, only the primary amine functional heterogeneous materials were investigated. However, little attention has been devoted to the optimum loading of other organoamines and its variation with the organoamine type.

In this paper, four amine functionalized mesoporous materials grafted by primary, dualistic and secondary amine groups were synthesized with different amine loading amounts. The materials were evaluated for the self-condensation reaction of *n*-butanal, a Knoevenagel condensation and a Henry reaction.

2 Experimental

2.1 Materials

MCM-41 in powder form was purchased from Shanghai Novel Chemistry Co., Ltd. (China). 3-Amino-propyltrimethoxysilane (APTS), 3-(*N*-methylaminopropyl)trimethoxysilane (MAPTS) and *N*-(2-aminoethyl)-3-aminopropyltrimethoxysilane (AAPTS) were obtained from Aladdin Reagent Co., Ltd. (China). Sodium borohydride, toluene, chloroform, benzaldehyde, absolute ethanol, *n*-butanal, 2-ethylhexenal and nitromethane were also obtained from Aladdin Reagent Co., Ltd. (China). Cyanoacetate and nitrostyrene were obtained from Sinopharm Chemical Reagent Co., Ltd. All reagents were used as received without any further purification.

2.2 Synthesis of amino-functionalized catalysts

The synthesis was conducted by stirring 1 g MCM-41 in various amounts of aminoorganosilanes (APTS, AAPTS or MAPTS) in 50 mL toluene at 110 °C for 15 h. The solution was filtered, washed repeatedly with dry toluene, followed by Soxhlet extraction with $CHCl_3$ to remove any organoamine adhered to the support walls with physisorption, and then dried at 80 °C overnight to get amino-functionalized catalysts. The resulting samples modified by APTS, AAPTS and MAPTS were designated as NH_2-MCM(x), NH_2NH-MCM(x), and $NHCH_3$-MCM(x) catalysts, respectively. Here, x denotes the added amine amount (mmol) for 1 g MCM-41 mesoporous silica.

Another type of secondary amino-functionalized catalysts was synthesized by a modified procedure in previous reports [41, 42] (Scheme 1). Benzaldehyde (5 mmol, 0.53 g) and APTS (5 mmol, 0.90 g) were refluxed in chloroform solution for 5 h. The obtained substance then reacted with 0.35 g $NaBH_4$ in absolute ethanol solution at room temperature for 18 h under intensive stirring. The requisite amount of MCM-41 was added and refluxed for 24 h. After the end of the reaction, the suspension was filtered, Soxhlet-

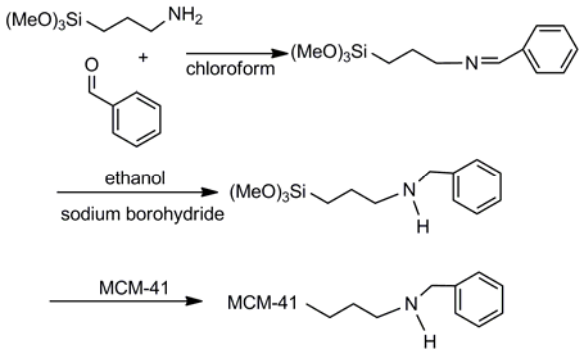

Scheme 1 Synthesis of NHPh-MCM.

extracted with $CHCl_3$, and then dried at 80 °C overnight. The obtained solid sample was suspended in 200 mL deionized water to remove excess sodium borohydride by hydrolysis reaction, and then filtered and dried. The obtained sample is a novel secondary amino-functionalized catalyst and denoted as NHPh-MCM-y. Here, y denotes the added MCM-41 mass (g).

2.3 Characterizations

2.3.1 FTIR

The Fourier Transform Infrared Spectrophotometer (FTIR) spectra of the as-synthesized catalysts were recorded with a Perkin-Elmer Spectrum Nicolet 5DX Fourier transform infrared spectrophotometer system in the region from 400 to 4000 cm^{-1} using KBr pellets.

2.3.2 N_2 adsorption and desorption

The N_2 adsorption-desorption measurements were carried out on a Micromeritics ASAP 2020 system at liquid N_2 temperature (−196 °C). Before measuring, the samples were degassed for 12 h at 105 °C.

2.3.3 XRD and elemental analysis

The powder X-ray diffraction patterns (XRD) were obtained by using a Scintag powder diffractometer. The elemental analysis was performed on a Perkin Elmer CHNS/O 2400 analyzer.

2.3.4 ^{13}C and ^{29}Si NMR

The solid-state ^{13}C (75.5 MHz) and ^{29}Si (59.6 MHz) NMR spectra were obtained on a Bruker AVANCE 300 NMR spectrometer. All spectra were measured at room temperature. For ^{13}C CP-MAS NMR experiments, a spin rate of 7.0 kHz, a recycle delay of 5 s and contact time of 1 ms were employed. For ^{29}Si CP-MAS NMR experiments, a spin rate of 7.0 kHz, a recycle delay of 10 s and contact time of 10 ms were employed.

2.4 Catalytic performances

The aldol self-condensation reaction of *n*-butanal (Scheme 2)

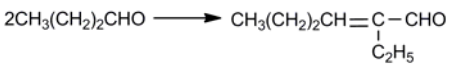

Scheme 2 Self-condensation reaction of *n*-butanal.

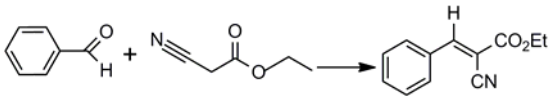

Scheme 3 Knoevenagel condensation.

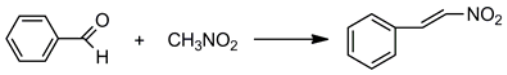

Scheme 4 Henry reaction.

was performed in a 30 mL magnetic stirring stainless steel reactor. 0.10 g catalyst, 10 mmol *n*-butanal (0.72 g) and 10 mL toluene as the solvent were added and nitrogen-sealed in the reactor. The reaction was performed at 110 °C for 11 h. After the reaction, the resulting mixtures were filtered and analyzed using gas chromatography (GC).

The Knoevenagel condensation reaction (Scheme 3) was performed as follows. 0.10 g catalyst, 5 mmol benzaldehyde (0.53 g), 5 mmol cyanoacetate (0.50 g) and 10 mL toluene as the solvent were added and nitrogen-sealed in the reactor. The reaction was performed at 110 ˚C for 11 h. After the reaction, the resulting mixtures were filtered and analyzed using gas chromatography (GC).

The Henry reaction (Scheme 4) was performed as follows: 0.10 g catalyst, 5 mmol benzaldehyde (0.53 g), and 10 mL nitromethane were added and nitrogen-sealed in the reactor. The reaction was performed at 110 °C for 11 h. After the reaction, the resulting mixtures were filtered and analyzed using gas chromatography (GC).

3 Results and discussion

3.1 Characterizations of the as-synthesized catalysts

Figure 1(a) illustrates the FTIR spectra of the functionalized mesoporous materials with different amine groups. The typical Si–O–Si bands around 1237, 1074, 800, and 457 cm^{-1} associated with the condensed silica network are presented in all cases. The presence of weak N–H bending vibration at 686 cm^{-1} for all samples and the symmetric $–NH^{3+}$ bending vibration around 1531 cm^{-1} for NH_2-MCM and NH_2NH-MCM confirms the incorporation of amino groups into the mesoporous silica. The weak bands between 1450 and 1475 cm^{-1} associated with $–CH_2–$ vibration and the peaks in the range of 2750–3000 cm^{-1} ascribed to the stretching of $–CH_2–$ groups can be observed for the samples containing aminopropyl groups. This further confirms the incorporation of organic species into MCM-41. The peak

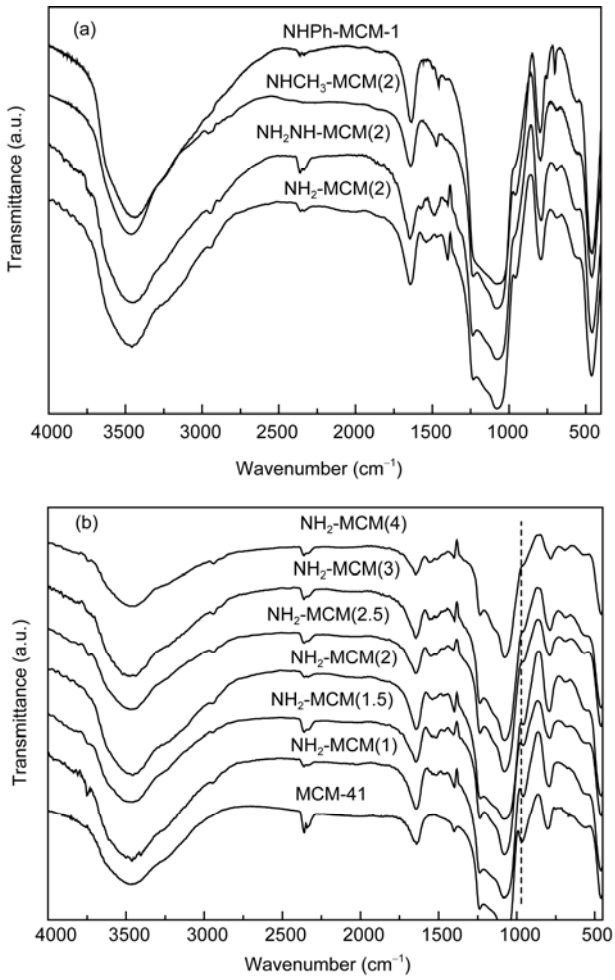

Figure 1 FTIR spectra of different organoamine functionalized mesoporous materials (a) and primary functionalized mesoporous materials with different amine contents (b).

around 1380–1430 cm^{-1} is due to the symmetric bending vibration of $–CH_3$ group from ethoxy moieties of aminosilane. For all samples, the strong peaks around 1630 cm^{-1} are ascribed to the bending vibration of adsorbed H_2O. The peaks associated with noncondensed Si–OH groups are present in the range of 940–970 cm^{-1} [23, 27, 43].

Figure 1(b) illustrates the FTIR spectra of the primary amine (APTS) functionalized mesoporous materials with different amine loading amounts. It shows clearly that the peak intensity of silanol groups decreases as the added APTS amount increases. Meanwhile, the gradual red shift of the silanol groups is observed as the APTS amount increases (indicated by a dashed line). It is the result of the increased interaction between the $–NH_2$ groups and the silanol groups through hydrogen bonding [23, 27].

The small angle XRD patterns of the amino-functionalized samples and MCM-41 are shown in Figure 2(a). The three well-defined peaks are indexed as (100), (110) and (200) planes, which are the typical P6mm honeycomb structure of the mesoporous support. These observable

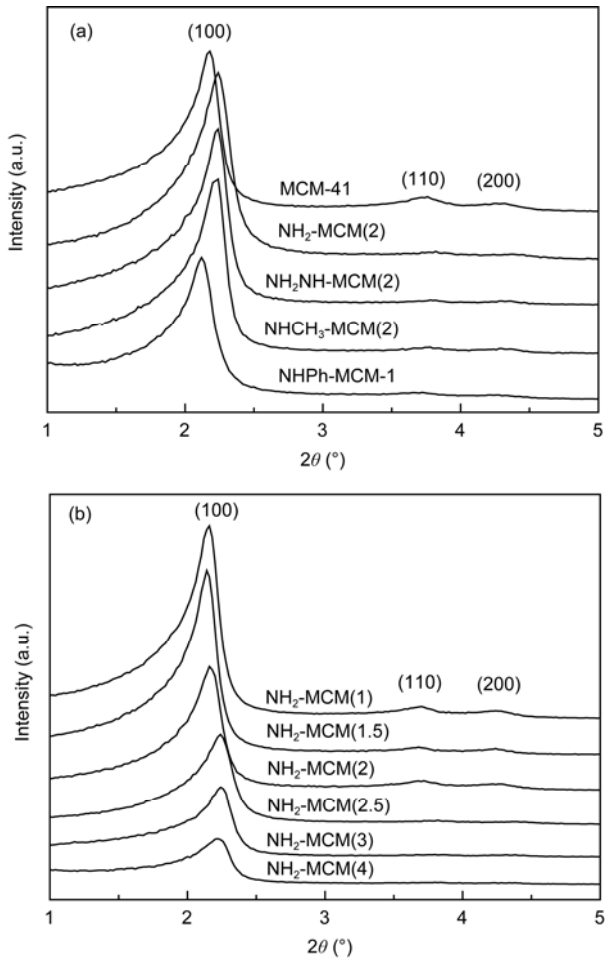

Figure 2 Powder X-ray diffraction (XRD) spectra of MCM-41 and different organoamine functionalized mesoporous materials (a) and primary functionalized mesoporous materials with different amine contents (b).

peaks indicate the stability of the original structure during the chemical modification process. However, the decrease in the intensity of the three peaks for the functionalized samples is observed, which suggests the formation of a less ordered mesoporous structure [34, 41]. Figure 2(b) shows the XRD patterns of NH_2-MCM samples grafted with different amounts of APTS. It is observed that the peak intensity decreases with the increase of the added APTS amount because the mesoporosity of the resulting catalysts decreases [24].

The surface areas, pore diameters and pore volume of the samples were characterized by N_2 adsorption-desorption experiments. The results are displayed in Table 1 and Figure 3. It is observed that all samples in type IV isotherms have mesoporous structures. In comparison with the original support MCM-41, the surface area, pore size, and pore volume of the amino-functional materials decrease. This further demonstrates the incorporation of organoamine into the framework of MCM-41 support [27].

Solid-state NMR analyses of NH_2-MCM(2), NH_2NH-MCM(1) and $NHCH_3$-MCM(1.5) were performed and their

Table 1 Structural properties of the amino-functionalized MCM-41

Sample	S_{BET} (m^2/g)	Pore size (nm)	Pore volume (mL/g)	Amine content (mmol/g)
MCM-41	872	3.17	0.82	–
NH_2-MCM(1)	771	2.89	0.67	0.84
NH_2-MCM(1.5)	755	2.87	0.66	1.26
NH_2-MCM(2)	754	2.64	0.54	1.49
NH_2-MCM(2.5)	663	2.41	0.48	1.91
NH_2-MCM(3)	595	2.30	0.43	2.22
NH_2-MCM(4)	269	1.76	0.23	2.72
NH_2NH-MCM(0.5)	826	2.93	0.70	0.51
NH_2NH-MCM(1)	760	2.89	0.64	0.85
NH_2NH-MCM(1.5)	699	2.30	0.54	1.19
NH_2NH-MCM(2)	689	2.14	0.48	1.56
NH_2NH-MCM(3)	467	1.97	0.30	2.01
$NHCH_3$-MCM(0.5)	854	2.94	0.72	0.48
$NHCH_3$-MCM(1)	800	2.93	0.64	0.78
$NHCH_3$-MCM(1.5)	804	2.77	0.58	1.21
$NHCH_3$-MCM(2)	749	2.38	0.49	1.59
$NHCH_3$-MCM(3)	654	1.91	0.46	2.34
NHPh-MCM-2	–	–	–	0.46
NHPh-MCM-1.5	–	–	–	0.56
NHPh-MCM-1.0	778	3.02	0.59	0.71
NHPh-MCM-0.6	–	–	–	0.89
NHPh-MCM-0.4	–	–	–	0.91

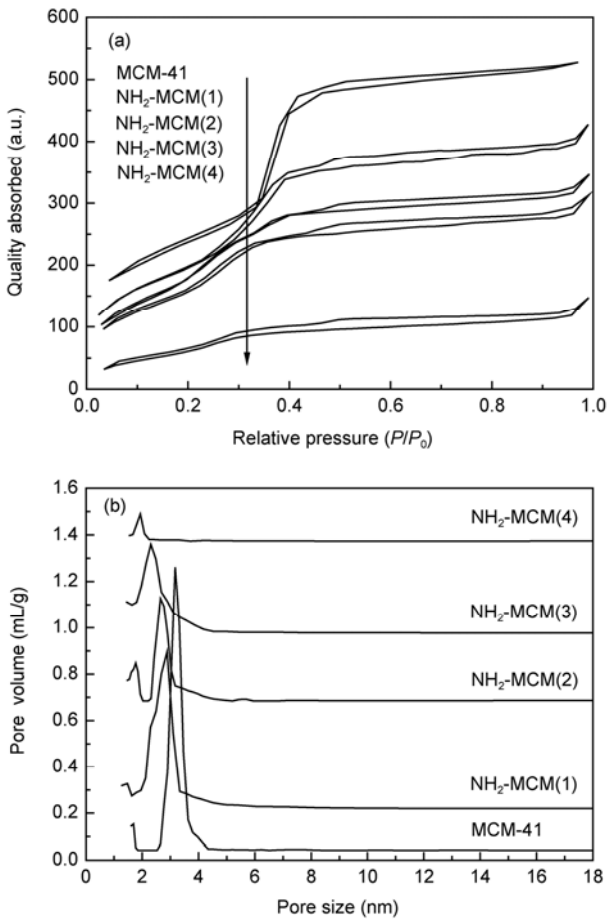

Figure 3 N_2 adsorption-desorption isotherms (a) and BJH pore-size distributions of MCM-41 and primary amine functionalized mesoporous materials with different amine contents (b).

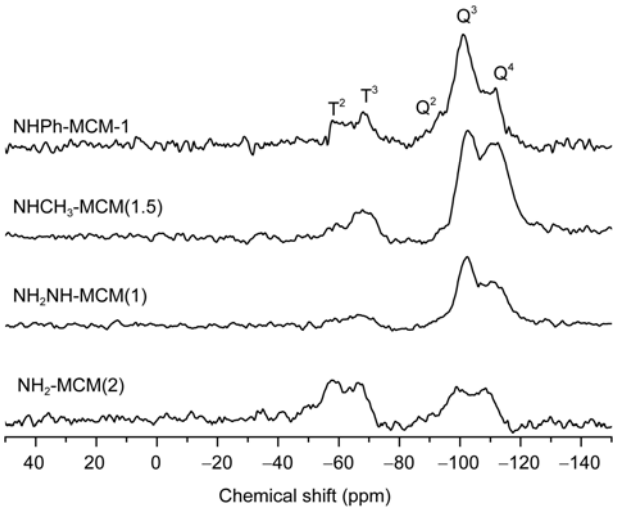

Figure 4 ^{29}Si CP MAS NMR spectra of different organoamine functionalized mesoporous materials.

chemical structures were investigated. Figure 4 shows the ^{29}Si CP MAS NMR spectra. Three clear resonance peaks derived from Q^n (Q^n = $Si(OSi)_n(OH)_{4-n}$, n = 2–4. Q^4: δ = −110 ppm; Q^3: δ = −100 ppm; Q^2: δ = −90 ppm) and two peaks derived from T^m (T^m = $RSi(OSi)_m(OH)_{3-m}$, m = 1–3. T^3: δ = −65 ppm; T^2: δ = −55 ppm; R: the grafted groups) are observed. The peaks indicate the introduction of an organic functional moiety into the silica skeleton [23, 24].

3.2 Catalytic performances

The catalytic performances of four organoamino-functionalized materials were firstly evaluated by the aldol self-condensation reaction of *n*-butanal. The variations of the 2-ethylhexenal yields with amine loading amounts for four catalysts are displayed in Figure 5. For each sample series, the 2-ethylhexenal yield firstly increases to a peak value and then decreases as the organoamine loading amount increases. Nevertheless, the amine loading amount of the peak point is apparently dependent on the loaded amine type. For NH_2-MCM sample series, the highest value is obtained with 1.49 mmol/g amine loading for the sample NH_2-MCM(2). For the samples of NH_2NH-MCM series, $NHCH_3$-MCM series and NHPh-MCM series, the highest values are obtained in amine loading of 0.84, 1.21 and 0.71 mmol/g, respectively. These results confirm the existence of an optimum amine loading amount as reported in the previous work [32]. At this point, the best acid-base synergetic effect is obtained between amine groups and the residual silanols. However, one can speculate that the yield decline for the catalysts with high amine loading may be due to the decrease of the surface area and pore size of the materials. To elucidate this doubt, Hruby *et al.* [33] shielded the residual silanols of the dihydroimidazole (DHIS) functionalized SBA-15 catalyst and compared the catalytic performances by the condensation reaction of ethyl cyanoacetate and benzaldehyde with toluene and methanol as the solvent, respectively. It was found that after silylation, the activity of the catalysts had a major decrease in toluene, but a minor decrease in methanol. This verified that the major activity decrease in toluene was mainly due to the miss of silanols rather than the decrease of the surface area and pore size.

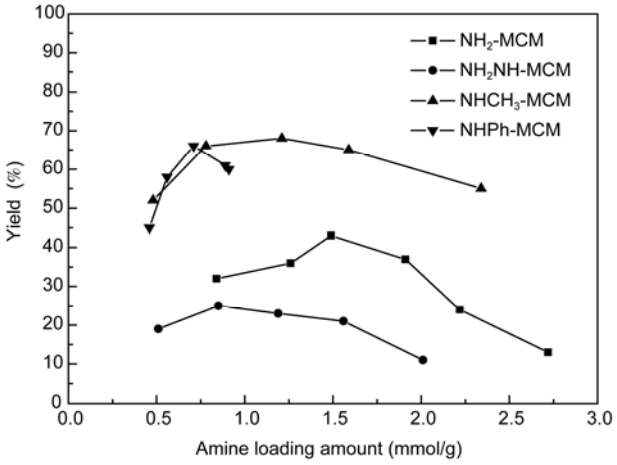

Figure 5 Yield of 2-ethylhexenal vs. amine loading plots for different amine functionalized catalysts.

Figure 5 shows an interesting phenomenon: the optimum amine loading amount for the different amine functionalized catalysts is closely related with the molecular volume of amine precursors. The optimum amine loading amount complies with the order of NH_2-MCM > $NHCH_3$-MCM > NH_2NH-MCM > NHPh-MCM. It is just opposite to the order of the molecular volume of the corresponding amine groups (NH_2– < $NHCH_3$– < NH_2NH– < NHPh–). Furthermore, a significant difference of the optimum amine loading point is found between two kinds of secondary amine functionalized catalysts. Additionally, it is noteworthy that the catalytic activity of NHPh-MCM varies more sharply in comparison with that of other catalysts with the variation of amine loading amount. This may be due to the more intense acid-base synergetic effect for NHPh-MCM catalysts. Because the amine group of NHPh– contains a large terminal, it can prevent the acid-base interaction between amines and silanols [41].

According to the above experimental results and the previous investigations [34], a mechanism is proposed to elucidate the influence of amine loading amount on the synergetic catalytic effect between organoamine groups and residual silanols in Figure 6. The surface silanol groups not only participate in the formation of the enamine intermediate but also facilitate the nucleophilic addition. Here, the secondary amine functionalized catalyst is used as an example. When the amine loading is low, the catalytic activity is low despite the much more silanol groups (Figure 6(a)). When the amine loading amount increases, the catalytic activity increases for the increased number of active sites. It is still surrounded by enough silanol groups. This synergis-

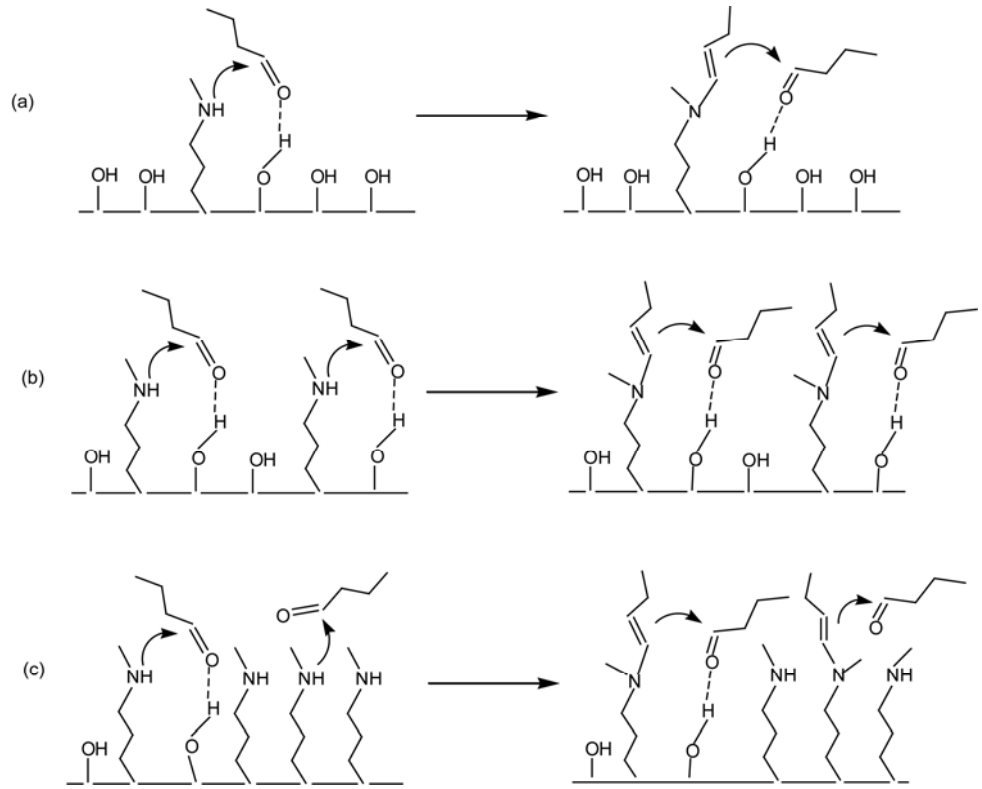

Figure 6 Acid-base synergetic mechanism in different amine loading for secondary amine functionalized catalysts.

tic effect produces better catalytic performances (Figure 6(b)). However, as the amine loading further increases, the samples have excessive amine groups and much less surface silanols. Thus, the catalytic performances evidently decrease because the synergetic effects are weakened for the lack of sufficient silanol groups (Figure 6(c)).

Considering the acid-base synergism, it is more reasonable to investigate the influences of the amine type on the catalytic performances of organoamine functionalized catalysts at each optimum amine loading point. According to this guideline, the catalytic performances of four as-synthesized catalysts with the optimum amine loading amounts for the self-condensation of *n*-butanal are evaluated and shown in Table 2. The results reveal that the secondary amine functionalized catalysts exhibit much better catalytic activity than that of primary and dualistic amine functionalized catalysts. This is probably due to the different catalytic mechanisms for different amines. The mechanism for the secondary amine functionalized catalysts involves an enamine intermediate formed between the aldehyde and amine group. However, in the cases of primary and dualistic amines, an imine intermediate is formed [40]. Meanwhile, in comparison with primary amine functionalized catalyst, dualistic amine functionalized catalyst has a similar TON value but lower yield. This may be due to the same catalytic mechanism for the primary amine functionalized catalyst, but its few active sites. When the two second amine functionalized catalysts are compared, the much higher TON and similar yield are obtained for NHPh-MCM catalyst although with rather fewer active sites than $NHCH_3$-MCM. NHPh-MCM catalyst has large organoamine terminal groups, which can restrict the acid-base combination between amine and silanol groups. Thus, more active amines and silanol groups can participate in the acid-base synergetic reaction and give a better catalytic activity.

Table 2 Catalytic self condensation reaction of *n*-butanal with different amine functionalized catalysts with optimum amine loading amounts

Entry	Catalyst	Yield (%)	TON [a)]
1	NH_2-MCM(2)	43	1.44
2	NH_2NH-MCM(1)	25	1.48
3	$NHCH_3$-MCM(1.5)	68	2.81
4	NHPh-MCM	66	4.65

a) Turnover number = mmol product/mmol organic groups per reaction time.

To investigate whether the diversity of acid-base synergism exits in different reactions, the catalytic performances of the second amine functionalized catalysts with varied amine loading amounts were also measured for the other two reactions, Knoevenagel condensation and Henry reaction, besides the self-condensation of *n*-butanal. The results are displayed in Figure 7. It shows that the optimum acid-base synergism points also exist for Knoevenagel condensation and Henry reactions, the same as the self-condensation reaction of *n*-butanal. Furthermore, the optimum amine loading amounts for three different reactions

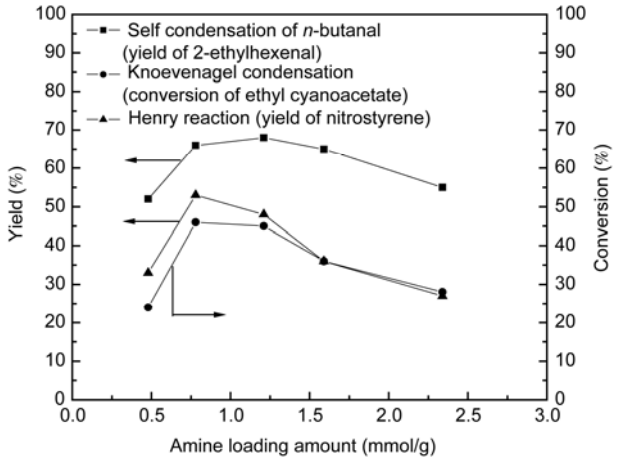

Figure 7 Performances of $NHCH_3$-MCM catalysts with different amine loading amounts in different reactions.

have little difference.

4 Conclusions

Four amine functional mesoporous catalysts were synthesized with MCM-41 as supports. By adjusting the organoamine precursor or support dosage, the amine loading amount and the residual silanols can be controlled. An optimum organoamine loading amount exists for each amine series catalysts. At the points, the best synergetic effects were obtained with the residual silanol groups. However, the optimum organoamine loading amount varies with the amine type and the terminal groups of the amine groups. The optimum organoamine loading amount has little difference for different reactions.

This work was supported by the National Natural Science Foundation of China (20906062) and Shanghai Municipal Natural Science Foundation (09ZR1423300).

1 Kresge CT, Leonowicz ME, Roth WG, Vartuli JC, Beck JS. Ordered mesoporous molecular sieves synthesized by a liquid-crystal template mechanism. *Nature*, 1992, 359: 710–712
2 Subba Rao YV, De Vos DE, Jacobs PA. 1,5,7-Triazabicyclo [4.4.0] dec-5-ene immobilized in MCM-41: A strongly basic porous catalyst. *Angew Chem Int Ed*, 1997, 36: 2661–2663
3 Shimizu K, Suzuki H, Hayashi E, Kodama T, Tsuchiya Y, Hagiwara H, Kitayama Y. Catalytic direct 1,4-conjugate addition of aldehydes to vinylketones on secondary-amines immobilised in FSM-16 silica. *Chem Commun*, 2002, 1068–1069
4 Inaki Y, Kajita Y, Yoshida H, Ito K, Hattori T. New basic mesoporous silica catalyst obtained by ammonia grafting. *Chem Commun*, 2001, 2358–2359
5 Yang Q, Kapoor MP, Shirokura N, Ohashi M, Inagaki S, Kondo JN, Domen K. Ethane-bridged hybrid mesoporous functionalized organosilicas with terminal sulfonic groups and their catalytic applications. *J Mater Chem*, 2005, 15: 666–673
6 Crieken RV, Melero JA, Morales G. Etherification of benzyl alcohols with 1-hexanol over organosulfonic acid mesostructured materials. *J Mol Catal A*, 2006, 256: 29–36
7 Inumaru K, Ishihara T, Kamiya Y, Okuhara T, Yamanaka S. Highly active solid acid catalysts composed of the keggin-type polyoxometalate $H_3PW_{12}O_{40}$ immobilized in hydrophobic nanospaces of organomodified mesoporous silica. *Angew Chem Int Ed*, 2007, 46: 7625–7628
8 Choudary BM, Lakshmi Kantam M, Sreekanth P, Bandopadhyay T. Knoevenagel and aldol condensations catalysed by a new diamino-functionalised mesoporous material. *J Mol Catal A*, 1999, 142: 361–365
9 Wight AP, Davis ME. Design and preparation of organic-inorganic hybrid catalysts. *Chem Rev*, 2002, 102: 3589–3614
10 De Vos DE, Dams M, Sels BF, Jacobs PA. Ordered mesoporous and microporous molecular sieves functionalized with transition metal complexes as catalysts for selective organic transformations. *Chem Rev*, 2002, 102: 3615–3640
11 Macquarrie DJ, Maggi R, Mazzacani A, Sartori G, Sartorio R. Understanding the influence of the immobilization procedure on the catalytic activity of aminopropylsilicas in C–C forming reactions. *Appl Catal A-Gen*, 2003, 246: 183–188
12 Árpád M, Bulcsú R. Organic transformations over silica materials modified by covalently bonded surface functional groups. *Curr Org Chem*, 2006, 10: 1697–1726
13 Angloher S, Kecht J, Bein T. Mesoporous ordered silica structures modified by metal organic reagents and their application in catalytic Michael additions. *Micropor Mesopor Mater*, 2008, 115: 629–633
14 Angeletti E, Canepa C, Martinetti G, Venturello P. Silica gel functionalized with amino groups as a new catalyst for Knoevenagel condensation under heterogeneous catalysis conditions. *Tetrahedron Lett*, 1988, 29: 2261–2264
15 Macquarrie DJ, Jackson DB. Aminopropylated MCMs as base catalysts: A comparison with aminopropylated silica. *Chem Commun*, 1997, 1781–1782
16 Kubota Y, Nishizaki Y, Ikeya H, Saeki M, Hida T, Kawazu S, Yoshida M, Fujii H, Sugi Y. Organic-silicate hybrid catalysts based on various defined structures for Knoevenagel condensation. *Micropor Mesopor Mater*, 2004, 70: 135–149
17 Wang XG, Lin KSK, Chan JCC, Cheng SF. Direct synthesis and catalytic applications of ordered large pore aminopropyl-functionalized SBA-15 mesoporous materials. *J Phys Chem B*, 2005, 109: 1763–1769
18 Bigi F, Carloni S, Maggi R, Mazzacani A, Sartori G. Nitroaldol condensation promoted by organic bases tethered to amorphous silica and MCM-41-type materials. *Stud Surf Sci Catal*, 2000, 130: 3501–3506
19 Demicheli G, Maggi R, Mazzacani A, Righi P, Sartori G, Bigi F. Supported organic catalysts: Synthesis of (*E*)-nitrostyrenes from nitroalkanes and aromatic aldehydes over propylamine supported on MCM-41 silica as a reusable catalyst. *Tetrahedron Lett*, 2001, 42: 2401–2403
20 Kubota Y, Goto K, Miyata S, Goto Y, Fukushima Y, Sugi Y. Enhanced effect of mesoporous silica on base-catalyzed aldol reaction. *Chem Lett*, 2003, 32: 234–235
21 Kubota Y, Ikeya H, Sugi Y, Yamada T, Tatsumi T. Organic-inorganic hybrid catalysts based on ordered porous structures for michael reaction. *J Mol Catal A*, 2006, 249: 181–190
22 Blanc AC, Macquarrie DJ, Valle S, Renard G, Quinn CR, Brunel D. The preparation and use of novel immobilised guanidine catalysts in base-catalysed epoxidation and condensation reactions. *Green Chem*, 2000, 2: 283–288
23 Wang XG, Tseng YH, Chan JCC, Cheng S. Catalytic applications of aminopropylated mesoporous silica prepared by a template-free route in flavanones synthesis. *J Catal*, 2005, 233: 266–275
24 Suzuki TM, Nakamura T, Fukumoto K, Yamamoto M, Akimoto Y, Yano K. Direct synthesis of amino-functionalized monodispersed mesoporous silica spheres and their catalytic activity for nitroaldol condensation. *J Mol Catal A : Chem*, 2008, 280: 224–232

25 Anan A, Sharma KK, Asefa T. Selective, efficient nanoporous catalysts for nitroaldol condensation: Co-placement of multiple site-isolated functional groups on mesoporous materials. *J Mol Catal A*, 2008, 288: 1–13
26 Su B, Lang WZ, Zeng QY, Liu XW, Yang CJ, Guo YJ. Preparation of organic functionalized mesoporous catalysts and their applications to the self-condensation reaction of *n*-butanal to 2-ethylhexenal. *Chin J Proc Eng*, 2010, 103: 55–360
27 Lang WZ, Liu XW, Guo YJ, Su B, Chu LF, Guo CX. A novel MCM-41-supported bi-functional catalyst by immobilizing organoamine and Rh-P complex for one-pot synthesis of 2-ethylhexenal from propene. *Micropor Mesopor Mater*, 2011, 142: 7–16
28 Shimizu KI, Hayashi E, Inokuchi T, Kodama T, Hagiwara H, Kitayama Y. Self-aldol condensation of unmodified aldehydes catalysed by secondary-amine immobilised in FSM-16 silica. *Tetrahedron Lett*, 2002, 43: 9073–9075
29 Bass JD, Solovyov A, Pascall AJ, Katz A. Acid–base bifunctional and dielectric outer-sphere effects in heterogeneous catalysis: A comparative investigation of model primary amine catalysts. *J Am Chem Soc*, 2006, 128: 3737–3747
30 Sharma KK, Asefa T. Efficient bifunctional nanocatalysts by simple postgrafting of spatially isolated catalytic groups on mesoporous materials. *Angew Chem Int Ed,* 2007, 119: 2879–2882
31 Sharma KK, Anan A, Buckley RP, Ouellette W, Asefa T. Toward efficient nanoporous catalysts: Controlling site-isolation and concentration of grafted catalytic sites on nanoporous materials with solvents and colorimetric elucidation of their site-isolation. *J Am Chem Soc*, 2008, 130: 218–228
32 Sharma KK, Buckley RP, Asefa T. Optimizing acid-base bifunctional mesoporous catalysts for the henry reaction: Effects of the surface density and site isolation of functional groups. *Langmuir*, 2008, 24: 14306–14320
33 Hruby SL, Shanks BH. Acid–base cooperativity in condensation reactions with functionalized mesoporous silica catalysts. *J Catal*, 2009, 263: 181–188
34 Xie YW, Sharma KK, Anan A, Wang G, Biradar AV, Asefa T. Efficient solid-base catalysts for aldol reaction by optimizing the density and type of organoamine groups on nanoporous silica. *J Catal*, 2009, 265: 131–140
35 Bass JD, Katz A. Bifunctional surface imprinting of silica: Thermolytic synthesis and characterization of discrete thiol-amine functional group pairs. *Chem Mater*, 2006, 18: 1611–1620
36 Notestein JM, Katz A. Enhancing heterogeneous catalysis through cooperative hybrid organic–inorganic interfaces. *Chem Eur J*, 2006, 12: 3954–3965
37 Zeidan RK, Hwang SJ, Davis ME. Multifunctional heterogeneous catalysts: SBA-15-containing primary amines and sulfonic acids. *Angew Chem Int Ed*, 2006, 45: 6332–6335
38 Zeidan RK, Davis ME. The effect of acid-base pairing on catalysis: An efficient acid-base functionalized catalyst for aldol condensation. *J Catal*, 2007, 247: 379–382
39 Motokura K, Tada M, Iwasawa Y. Heterogeneous organic base-catalyzed reactions enhanced by acid supports. *J Am Chem Soc*, 2007, 129: 9540–9541
40 Shylesh S, Wagner A, Seifert A, Ernst S, Thiel WR. Cooperative acid-base effects with functionalized mesoporous silica nanoparticles: Applications in carbon–carbon bond-formation reactions. *Chem Eur J*, 2009, 15: 7052–7062
41 Shao YQ, Guan JQ, Wu SJ, Liu H, Liu B, Kan QB. Synthesis, characterization and catalytic activity of acid–base bifunctional materials by controlling steric hindrance. *Micropor Mesopor Mater*, 2010, 128: 120–125
42 Cousinié S, Gressier M, Alphonse P, Menu MJ. Silica-based nanohybrids containing dipyridine, urethan, or urea derivatives. *Chem Mater*, 2007, 19: 6492–6503
43 Kim JY, Seidler P, Wan LS, Fil C. Formation, structure, and reactivity of amino-terminated organic films on silicon substrates. *Colloid Interf Sci*, 2009, 329: 114–119